Int. J. of GEOMATE, March, 2014, Vol. 6, No. 1 (Sl. No. 11), pp. 763-770
Geotech., Const. Mat. and Env., ISSN:2186-2982(P), 2186-2990(O), Japan

EFFECT OF STIFFNESS OF THIN BEARING LAYER ON TOE BEARING MECHANISM OF STEEL PIPE PILE WITH A CONCRETE BULB

Kazuhiro Oda[1], Shuhei Takegawa[2]

[1, 2] Graduate School of Engineering, Osaka University, Japan

ABSTRACT: It has been known that the sufficiently stiff layer can be considered as a load-bearing layer of piles, even if its thickness is thin. The authors have studied the toe bearing resistance of pile on a thin load-bearing layer, in order to establish the design method about pile on a thin load-bearing layer. In this paper, the effect of stiffness of load-bearing layer on characteristics of toe resistance of steel pipe pile on a thin load-bearing layer is discussed through a series of numerical analyses. First, a field loading test of steel pipe piles with a concrete bulb on a thin load-bearing layer is reproduced through the numerical analysis, in which a soil-water coupled with an elast-plastic finite element method is applied, to confirm the availability of the numerical analysis proposed. Second, a series of numerical analyses are carried out in which the deformation modulus of the load-bearing layer and the thickness of load-bearing layer are chosen as a variable parameter. The results of the numerical analyses show that the stiffness of load-bearing layer affects the resistance when the yielding of load-bearing layer occurs.

Keywords: Steel pipe pile, Stiffness of load-bearing layer, Load-bearing resistance at the pile toe, Thin load-bearing layer, Numerical analyses

1. INTRODUCTION

Most big cities in Japan have been constructed on Holocene plains. In general, such plains are composed of sand or sandy gravel layers and thick clay layers what accumulated alternatively. A stiff and thick layer which can be considered as load-bearing layer for piles could not be found in many cases. In particular, it has become more difficult to find a sufficiently stiff and thick load-bearing layer because a large number of pile foundations with large diameters have been constructed recently.

The appropriate estimation of toe bearing resistance of pile on a thin load-bearing layer can give the economical advantage for construction of pile foundations. The authors have studied the characteristics of toe bearing resistance of pile on a thin load-bearing layer in order to establish the design method about pile on a thin load-bearing layer. It is elucidated that the toe bearing resistance of pile on a thin load-bearing layer is affected significantly by the thickness of load-bearing layer in the case where it is less than 3 times pile diameter. Also, the yielding of thin load-bearing layer must be dominated by the punching shear failure [1], [2], [3].

In this paper, the effect of stiffness of load-bearing layer on the characteristics of toe resistance of pile on a thin load-bearing layer is elucidated through a series of numerical analyses. First, a field loading test of steel pipe piles with a concrete bulb on a thin load-bearing layer is reproduced through the numerical analysis, in which a soil-water coupled with an elasto-plastic finite element method is applied. Second, a series of numerical analyses are carried out in which the deformation modulus and the thickness of the load-bearing layer are chosen as a variable parameter. The effect of stiffness of load-bearing layer on characteristics of toe bearing resistance of pile on a thin load-bearing layer is discussed by focusing on both the relationship resistance and displacement at pile toe and the development of local failure in the bearing ground.

2. NUMERICAL ANALYSIS

2.1 Field Loading Test

Figure 1 shows the configuration of the instruments that were used to measure the displacement of pile with a concrete bulb, the displacements of bearing ground below the concrete bulb, and the axial force [4]. As shown in Fig.1 (a), a standard penetration test (SPT) was carried out to investigate the ground conditions at the southeast part of the Osaka Bay area. Based on the results of the SPT, it was found that the ground is composed of alternate layers of clay and sand or sandy gravel. The sand layers that show an N-value of more than 50 in the SPT were found to have a thickness of less than 2 m, which indicates that no clear load-bearing layer is available.

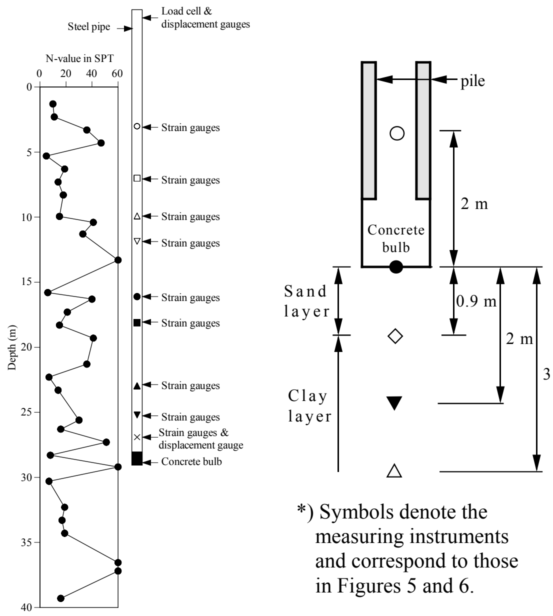

a) Strain gauges around pile shaft, load cell, and displacement gauges

b) Wire-type displacement gauges in the ground

Fig.1 Configuration of instruments used to measure the displacement of pile with concrete bulb, the displacements of the bearing ground below the concrete bulb, and the axial force

The tested pile was a steel pipe that is 34 m in length and 1 m in diameter, D, with a concrete bulb that is 1 m in length and 1 m in diameter. The length of the embedded part of the pile is about 27.9 m. The pile was born on a sand layer that is 0.9 m thick, which is underlain by a stiff clay layer. First, the pile was installed by a combination of inner excavation and penetration into the ground, until the pile toe reached the bearing ground. Second, the ground below the pile toe was excavated and a cavity was created in the bearing ground. Third, a cement mix with high pressure of about 20 MPa was injected into the cavity, creating a concrete bulb below the pile toe.

The load and displacement at the pile head were measured by a load cell and a displacement gauge. A displacement gauge was also set up at the pile toe. The displacements of the concrete bulb and the bearing ground below the concrete bulb were measured by wire-type displacement gauges. Strain gauges were also set up around the pile shaft. The axial force, which is denoted by symbols, was calculated from the measured strain. The axial force, which was calculated from the measurements of the strain gauges closest to the pile toe, was defined as the pile toe load.

2.2 Analytical Model

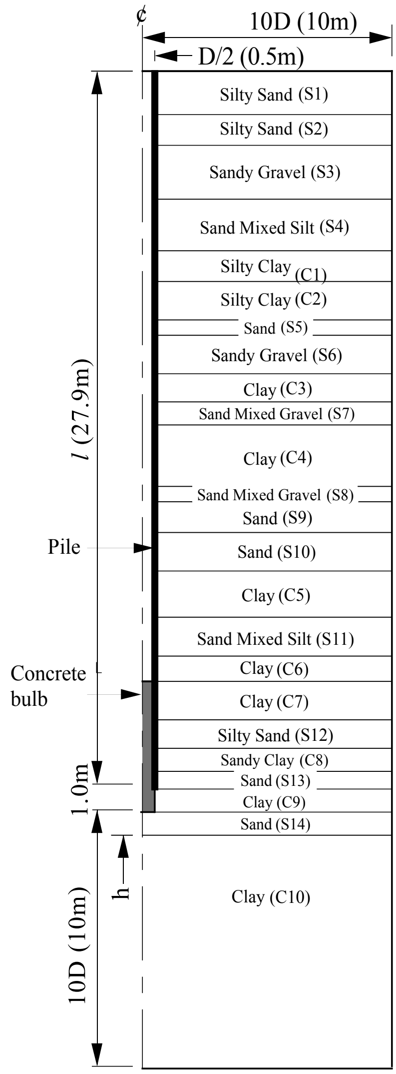

Fig.2 Analytical model

A soil-water coupled elasto-plastic finite element method with an axisymmetric condition was used in the numerical analysis. Figure 2 and Table 1 show the analytical model and the values of the soil parameters used in the analysis, respectively. The soils were fundamentally modeled as elasto-plastic materials to realistically reproduce the complicated behavior of the ground. The steel pipe pile and the concrete bulb were modeled as being composed of elastic materials. For almost all sandy soils, the tij-sand model, which was proposed by Nakai [5], was used, provided that soil stresses did not reach the failure threshold of the model. When the stresses did reach the failure threshold, the constitutive model of sandy soils was replaced with the Drucker-Prager model. For clayey soils, an elasto-plastic model proposed by Matsui and Abe [6] was used. When the stresses reached the failure threshold of the elasto-plastic model, the constitutive model of clayey soils was replaced with the von Mises model. A joint element proposed by Goodman et al.

Table 1 Values of soil parameters used in the analysis

Division	Model	Parameters
S1	Elasticity	$E = 18.9$ MPa, $\nu = 0.2$
S2	Elasticity 2	$E = 37.8$ MPa, $\nu = 0.2$
S3	Elasticity 3	$E = 72.5$ MPa, $\nu = 0.2$
S4	Elasticity 4	$E = 15.8$ MPa, $\nu = 0.2$
C1	Elasticity 5	$E = 18.9$ MPa, $\nu = 0.2$
C2	Elasticity 6	$E = 25.2$ MPa, $\nu = 0.2$
S5	Elasticity 7	$E = 31.5$ MPa, $\nu = 0.2$
S6	Elasticity 8	$E = 72.5$ MPa, $\nu = 0.2$
C3	Matsui-Abe model	$\lambda = 0.0360$, $\kappa = 0.00899$, $M = 1.635$, $\nu = 1/3$, $\eta_{k0} = 0.75$
S7	tij-sand model	$C_t = 8.77 \times 10^{-3}$, $C_e = 6.20 \times 10^{-3}$, $m = 0.3$, $\alpha = 0.90$, $R_e = 5.83$, $D_f = -0.36$, $\nu = 0.325$
C4	Matsui-Abe model	$\lambda = 0.0450$, $\kappa = 0.00563$, $M = 1.551$, $\nu = 1/3$, $\eta_{k0} = 0.75$
S8	tij-sand model	$C_t = 1.90 \times 10^{-2}$, $C_e = 1.35 \times 10^{-2}$, $m = 0.3$, $\alpha = 0.85$, $R_e = 4.49$, $D_f = -0.3$, $\nu = 0.325$
S9	tij-sand model	$C_t = 5.93 \times 10^{-2}$, $C_e = 4.19 \times 10^{-2}$, $m = 0.3$, $\alpha = 0.65$, $R_e = 3.36$, $D_f = -0.15$, $\nu = 0.325$
S10	tij-sand model	$C_t = 2.56 \times 10^{-2}$, $C_e = 1.48 \times 10^{-2}$, $m = 0.3$, $\alpha = 0.85$, $R_e = 4.56$, $D_f = -0.20$, $\nu = 0.325$
C5	Matsui-Abe model	$\lambda = 0.0257$, $\kappa = 0.00642$, $M = 1.551$, $\nu = 1/3$, $\eta_{k0} = 0.75$
S11	tij-sand model	$C_t = 6.43 \times 10^{-2}$, $C_e = 3.71 \times 10^{-2}$, $m = 0.3$, $\alpha = 0.55$, $R_e = 2.49$, $D_f = -0.15$, $\nu = 0.325$
C6	Matsui-Abe model	$\lambda = 0.0692$, $\kappa = 0.0173$, $M = 1.179$, $\nu = 1/3$, $\eta_{k0} = 0.75$
C7	Matsui-Abe model	$\lambda = 0.0309$, $\kappa = 0.00773$, $M = 1.551$, $\nu = 1/3$, $\eta_{k0} = 0.75$
S12	tij-sand model 6	$C_t = 4.80 \times 10^{-2}$, $C_e = 2.77 \times 10^{-2}$, $m = 0.3$, $\alpha = 0.75$, $R_e = 3.89$, $D_f = -0.18$, $\nu = 0.325$
C8	Matsui-Abe model	$\lambda = 0.0592$, $\kappa = 0.0148$, $M = 1.221$, $\nu = 1/3$, $\eta_{k0} = 0.75$
S13	tij-sand model	$C_t = 5.99 \times 10^{-2}$, $C_e = 4.14 \times 10^{-2}$, $m = 0.3$, $\alpha = 0.80$, $R_e = 4.02$, $D_f = -0.20$, $\nu = 0.325$
C9	Matsui-Abe model	$\lambda = 0.1021$, $\kappa = 0.00681$, $M = 1.551$, $\nu = 1/3$, $\eta_{k0} = 0.75$
S14	tij-sand model	$C_e = 4.94 \times 10^{-2}$, $m = 0.3$, $\alpha = 0.90$, $R_e = 4.60$, $D_f = -0.45$, $\nu = 0.325$
C10	Matsui-Abe model	$\lambda = 0.247$, $\kappa = 0.0124$, $M = 1.418$, $\nu = 1/3$, $\eta_{k0} = 0.75$

[7] was used to represent the discontinuity between pile and soil.

The soil parameters used in the numerical analysis were determined from data from soil investigations that included the SPT and unconfined compression test. Few parameters were reasonably rearranged to fit the results of the numerical analysis to the field measurements.

2.3 Verification of Numerical Analysis

Figure 3 shows the relationship between the applied load and the displacement at the pile head. In the analytical relationship between the applied load and displacement, the slope of the analytical curve changes at about 3 MN of the applied load at the pile head. Then, the slope of analytical curve becomes gradually steeper with an increase in the applied load at the pile head. Finally, the analytical displacement of the pile head significantly increases at an applied load of about 4.8 MN. It is considered that the resistance of the pile head at this load level is closer to the ultimate bearing resistance of the test pile.

Figure 4 shows the relationship between the

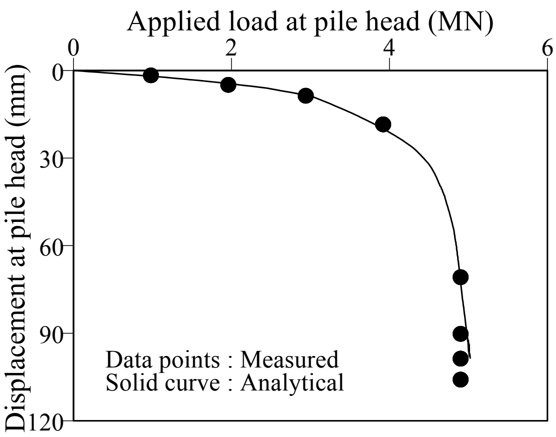

Fig.3 Relationship between applied load and displacement at pile head

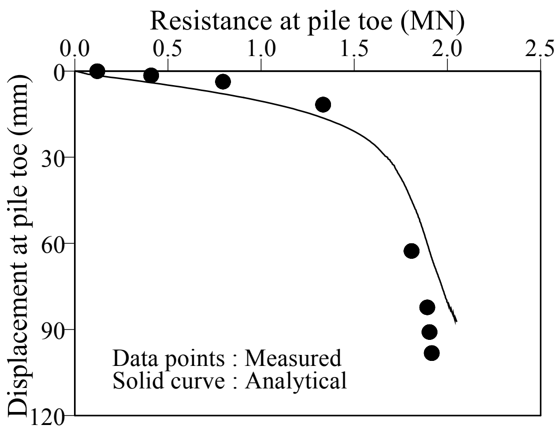

Fig.4 Relationship between resistance and displacement at pile toe

resistance and displacement at the pile toe. The slope of the analytical curve hardly changes up to a resistance of about 1.8 MN. The analytical displacement then significantly increases at a load level of about 1.8 MN. It is found that the yield of the resistance and displacement behavior at the pile toe occurs at this load level.

Figure 5 shows the axial force distribution of the test pile. The numerical analysis reasonably reproduces the friction behavior around the pile shaft.

Figure 6 shows the relationship between the resistance at the pile toe and the displacements in the underlying bearing ground, in addition to that of the concrete bulb. The analytical relationship between the resistance and displacement, which is indicated by a solid circle at the toe of the concrete bulb, agrees closely with that which is indicated by an empty circle at the inner concrete bulb, indicating that the concrete bulb acts in coordination with the steel pipe piles. In addition, it is considered that failure of the concrete bulb did not occur. It should be noted that the displacement at a point 1 m below the toe of the concrete bulb, i.e., at the bottom of the sand layer, which is denoted by an open rhombus, increases more significantly than that at the point 2 m below the toe, which is denoted by a solid triangle, as the resistance and displacement behaviors at the pile toe begin to yield.

As shown in Figures 3, 4, 5 and 6, the agreement between the measured and analytical results is good, thus confirming that the numerical analysis realistically reproduces the bearing behavior of the pile and the foundation behavior of the ground around the pile toe in the field loading test [2].

Figure 7 shows the analytical results of the deformation of the bearing ground below the concrete bulb in the final stage of loading. The bearing ground behaves as if the pile might punch through the thin load-bearing layer. In particular, the finite elements of the thin load-bearing layer directly below the perimeter of the concrete bulb deform as if they were subject to simple shearing. This suggests that the punching shear failure occurs in the bearing ground below the concrete bulb.

3. EFFECT OF STIFFNESS OF LOAD-BEARING LAYER ON BEARING CHARACTERISTICS AT PILE TOE

3.1 Analytical Cases

Table 2 shows the analytical cases in the parametric study. In this paper, the stiffness of load-bearing layer could be considered as the compressibility of sands or sandy gravels which

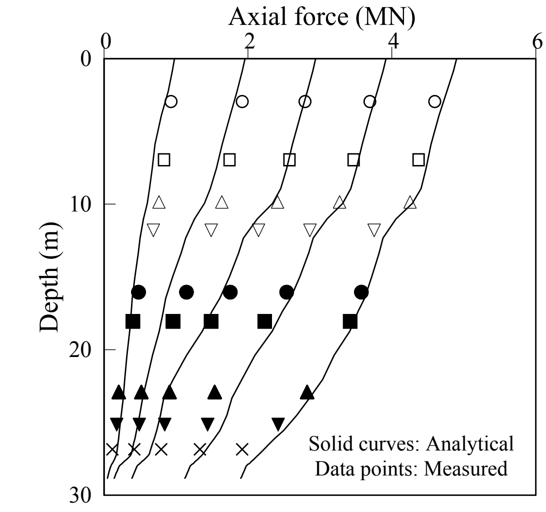

Fig.5 Axial force distribution of pile

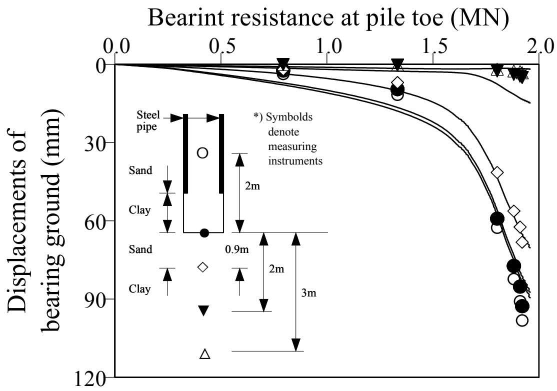

Fig.6 Relationship between resistance at pile toe and displacement of the concrete bulb and underlying bearing ground

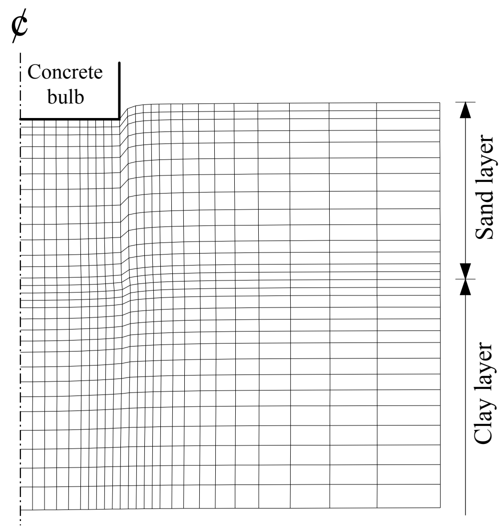

Fig.7 Analytical results of the deformation of bearing ground around concrete bulb at the final stage of loading

Table 2 Analytical cases

Case	Deformation modulus	C_t	Thickness of bearing layer
E1014h15	1014 kgf/cm^2	5.69×10^{-3}	1.5m
E830h15	830 kgf/cm^2	6.95×10^{-3}	1.5m
E670h15	670 kgf/cm^2	8.60×10^{-3}	1.5m
E1014h25	1014 kgf/cm^2	5.69×10^{-3}	2.5m
E830h25	830 kgf/cm^2	6.95×10^{-3}	2.5m
E670h25	670 kgf/cm^2	8.60×10^{-3}	2.5m

forms the load-bearing layer. C_t, which is one of the most important parameters in tij-sand model, was chosen as variable parameter, in order to change the deformation modulus of the load-bearing layer. C_t is mechanical parameter for controlling the volumetric compression behavior. The volumetric strain rate, $\dot{\varepsilon}_{vol}$, can be defined by the following equation.

$$\dot{\varepsilon}_{vol} = m C_t p'^{m-1} \dot{p}' \quad (1)$$

where p' is mean principal stress at the initial condition and m is a material parameter. Also, the dot denotes the rate. On the other hand, the volumetric strain rate in the elastic media is defined by the Eq. (2).

$$\dot{\varepsilon}_{vol} = K\dot{p}' \quad (2)$$

where K is bulk modulus. Also, K can be given by the following equation.

$$K = \frac{E}{3(1-2v)} \quad (3)$$

where E is deformation modulus and v is poisson's ratio. From Eq. (1), Eq. (2) and Eq. (3), E is given by

$$E = 3(1-2v) m C_t p'^{m-1} \quad (4)$$

Strictly speaking, E does not imply the elastic modulus in this paper.

Also, in the analyses, the thickness of load-bearing layer, h, was chosen as 1.5m and 2.5m

3.2 Relationship between Resistance and Displacement at Pile Toe

Figure 8 shows the relationship between resistance and displacement at pile toe in the case where the thickness of the load-bearing layer is equal to 1.5m (h/D = 1.5). The resistance at pile toe increases as the deformation modulus of load-bearing layer is greater at the same displacement before the yielding of the relationship between resistance and displacement at pile toe occurs. In the case of E1014h15, the yielding in relationship between resistance and displacement at pile toe occurs at toe displacement of about 4.0cm and at toe resistance of about 2.8MN. Also, in the case of E830h15, the yielding in relationship between resistance and displacement at pile toe occurs at toe displacement of about 8.0cm and at toe resistance of about 3.1MN. However, in the case of E670h15, the yielding does not occur until the displacement at pile toe reaches 10cm which is equal to 10% of the pile diameter. In general, the toe resistance at the displacement of 10% of pile diameter can be estimated as the ultimate bearing resistance in design method, in Japan. The yielding occurs at the toe displacement of about 12cm and at toe resistance of 3.3MN in the case of E670h15. After the yielding occurs, the resistance at pile toe hardly increases with the displacement in each analytical case. Also, the resistance at pile toe in each case is closely agreed with those in the other cases at the displacement of 15cm.

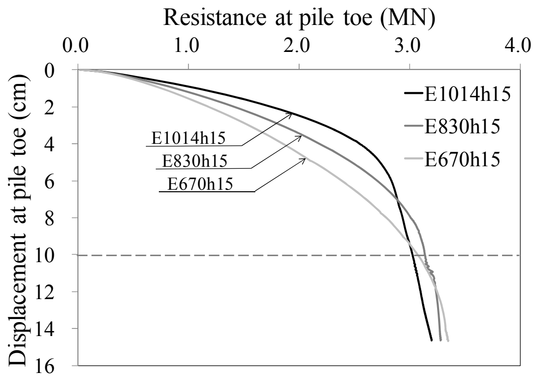

Fig.8 Relationship between resistance and displacement at pile toe (h/D = 1.5)

Figure 9 shows the relationship between resistance and displacement at pile toe in the case where the thickness of the load-bearing layer is equal to 2.5m (h/D = 2.5). In all cases, the resistance at pile toe is greater than the relationship between resistance and displacement at pile toe in the case where the thickness of the load-bearing layer is equal to 1.5m. The resistance at pile toe increases as the deformation modulus of load-bearing layer is greater at the same displacement. In the case of E1014h25, the yielding of relationship between resistance and displacement at pile toe occurs at toe displacement of about 8.0cm and at toe resistance of about 4.8MN. However, in cases of E830h25 and E670h25, the yielding does not occur until at the displacement at pile toe reaches 10cm.

3.3 Development of Local Failure in Bearing Ground

Figure 10 shows the development of local failure in bearing ground underneath a concrete bulb in the case where the thickness of the load-bearing layer is equal to 1.5m (h/D = 1.5). In figure 10, the zone in which the local failure occurs is painted red. In E1014h15, the local failure zone surrounds the compressed zone underneath the toe of concrete bulb in the load-bearing layer and reaches nearly the clay layer underlying the load-bearing layer at toe displacement of 4cm. The yielding of relationship between resistance and displacement at pile toe occurs at toe displacement of about 4cm in E1014h15, as shown in Fig.8. It is, therefore, suggested that the punching shear failure, in which a highly compacted core of soils is formed underneath a concrete bulb due to the installing the pile into the load-bearing layer, is the prevailing bearing mechanism.

In E830h15, the local failure develops slowly than in E1014h15. The local failure zone does not reach the clay layer underlying load-bearing layer at toe displacement of 4cm surrounding the compressed zone underneath the toe of concrete bulb. The failure zone in the bearing layer reaches nearly the clay layer underlying at toe displacement of 8cm. At toe displacement of

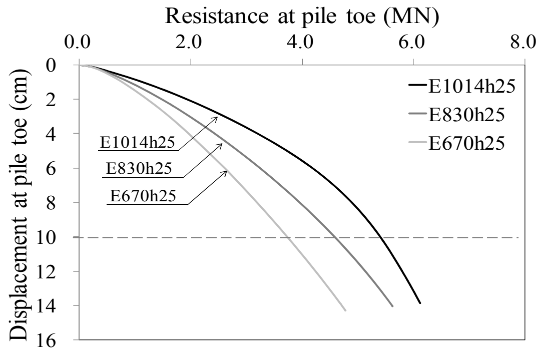

Fig.9 Relationship between resistance and displacement at pile toe (h/D = 2.5)

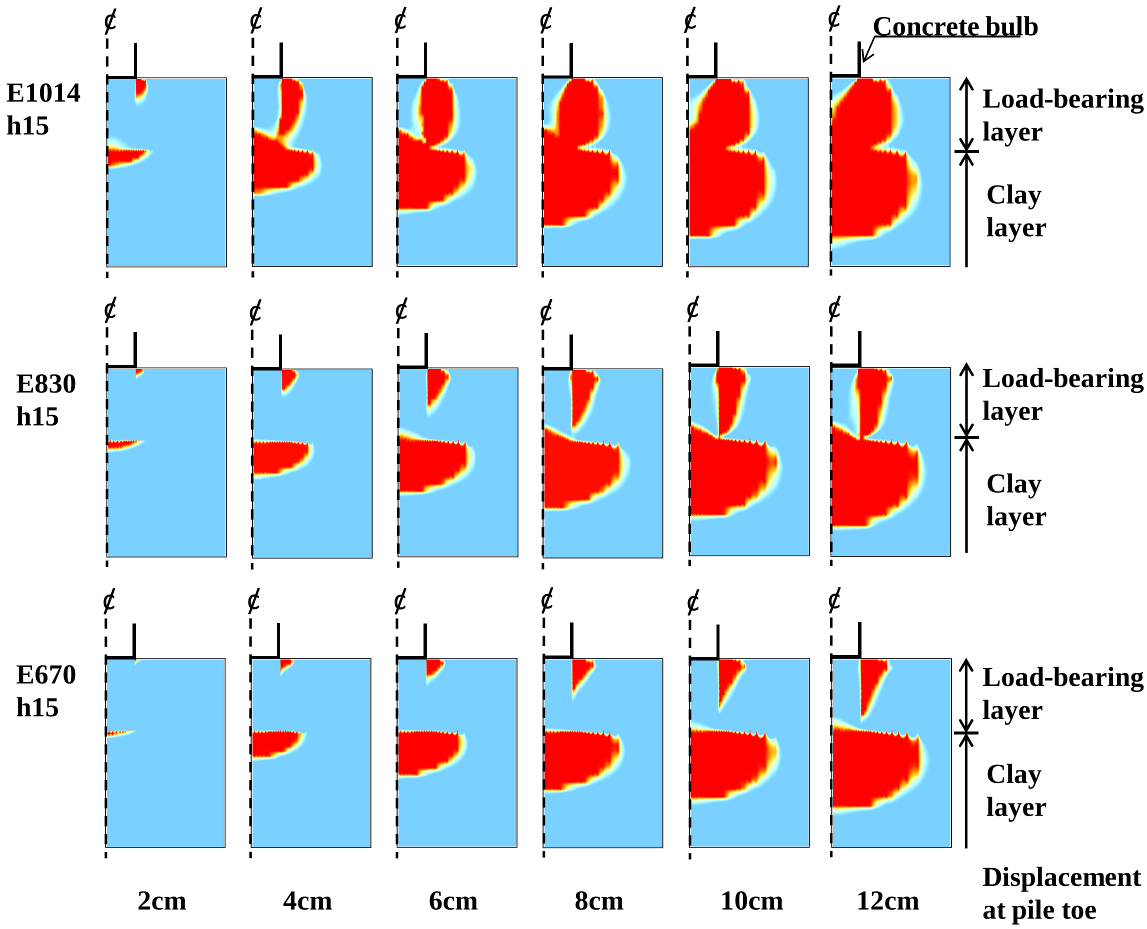

Fig.10 Development of local failure in bearing ground underneath a concrete bulb (h/D =1.5)

about 8cm, the occurrence of yielding is confirmed as shown in Fig.8. It is suggested that punching shear failure is the prevailing bearing mechanism in E830h15, too.

In E670h15, the local failure zone surrounding the compressed zone underneath the toe of concrete bulb reaches nearly the clay layer underlying the load-bearing layer at toe displacement of 12cm.

Figure 11 shows the development of local failure in bearing ground underneath a concrete bulb in the case where the thickness of the load-bearing layer is equal to 2.5m (h/D = 2.5). In E1014h25, the local failure zone surrounds the compressed zone underneath the toe of concrete bulb in the load-bearing layer and reaches nearly the clay layer underlying the load-bearing layer at toe displacement of 8cm. The yielding of relationship between resistance and displacement at pile toe occurs at toe displacement of about 8cm in E1014h25, as shown in Fig.9. It is, therefore, suggested that the punching shear failure is the prevailing bearing mechanism.

However, in E830h25 and E670h25, the local failure zone surrounding the compressed zone underneath the toe of concrete bulb does not reach the clay layer underlying the load-bearing layer at toe displacement of 10cm. It is, therefore, suggested that the punching shear failure does not occur in both case of E830h25 and E670h25. Consequently, the resistance at pile toe can depends significantly the stiffness of load-bearing layer.

4. CONCLUSIONS

In this study, the effect of stiffness of load-bearing layer on bearing characteristics of a steel pipe pile with concrete bulb on a thin load-bearing layer was investigated through a series of numerical analyses. The main conclusions are summarized as follows.

1. The numerical analysis which was developed by authors, realistically reproduces the bearing behavior of the steel pipe pile with concrete bulb on a thin load-bearing layer in a field loading test.
2. The resistance at pile toe increases as the stiffness of load-bearing layer is higher at the same level of displacement before the yielding of relationship between resistance and displacement at pile toe occur.
3. The resistance at pile toe at the displacement of

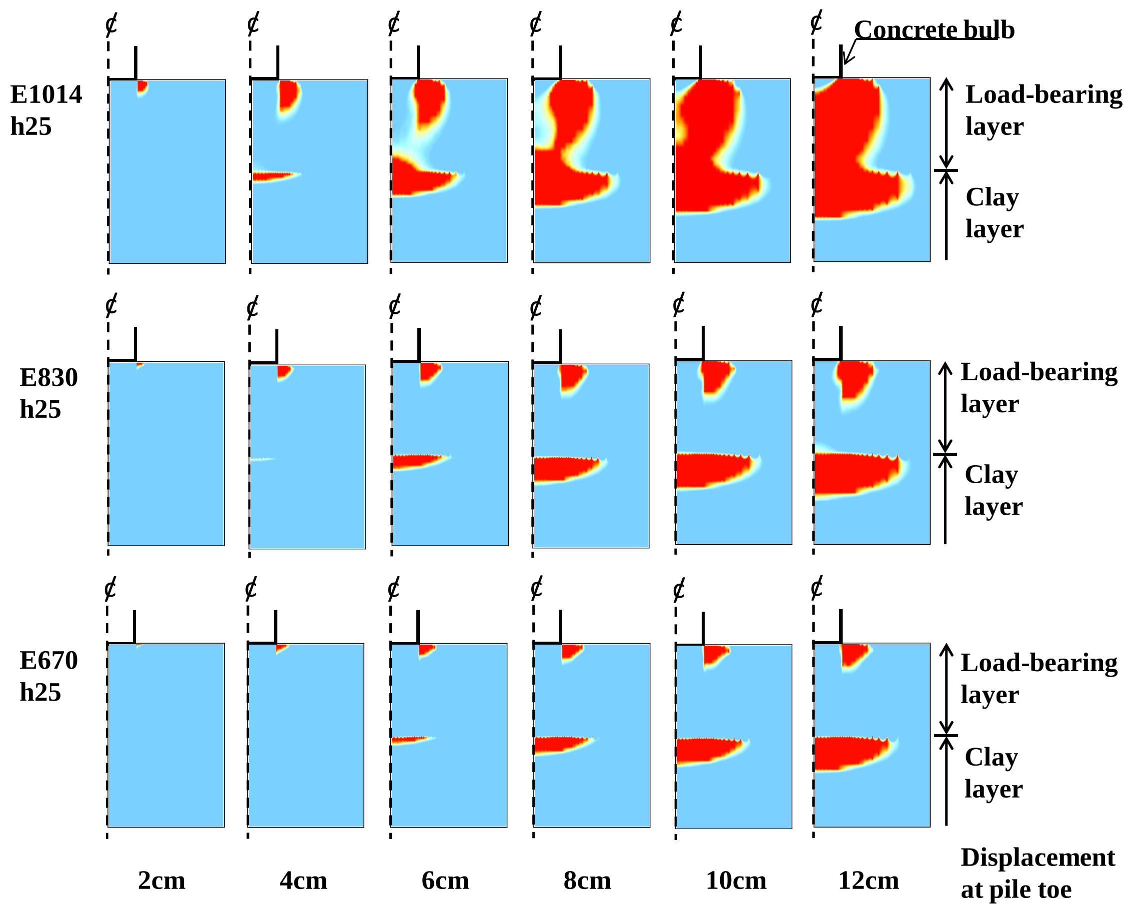

Fig.11 Development of local failure in bearing ground underneath a concrete bulb (h/D =2.5)

10% of pile diameter might be not significantly affected by the stiffness of load-bearing layer, in the case where the thickness of load-bearing layer is equal to 1.5m.
4. The punching shear failure is the prevailing bearing mechanism, regardless of the stiffness of load-bearing layer, in the case where the thickness of load-bearing layer is equal to1.5m.
5. The resistance at pile toe at the displacement of 10% of pile diameter is affected by the stiffness of load-bearing layer. The stiffer the load-bearing layer is, the greater the resistance at pile toe is.
6. The punching shear failure does not occur in the case of E830h25 and E670h25. The resistance at pile toe depends significantly the stiffness of load-bearing layer.

5. ACKNOWLEDGEMENT

The authors would particularly like to thank the Japan Iron and Steel Federation for scholarship.

6. REFERENCES

[1] Matsui, T., K. Oda, and M. Nakabayashi, “End bearing mechanism of bored pile on thin bearing layer”, Proceedings of 9th Asian Regional Conference on Soil Mechanics and Foundation Engineering, Vol. 1, 1991, pp.251-254.
[2] Matsui, T., K. Oda, and M. Nakabayashi, “Deformation behavior of bored steel pipe piles with concrete bulb on a thin bearing layer”, Proceedings of the 4th International Offshore and Polar Engineering Conference, 1994, pp.548-553.
[3] Takegawa, S., Oda, K., Ikefuji, Y., “Effect of strength of bored steel pile pipes with concrete bulb on end bearing characteristics on a thin layer”, Proc. 47th annual meeting of J.G.S, 2012, pp. 1075-1076.
[4] Koike, M., F. Yasuda, T. Takasuga, and T. Katayama, “Loading test of large-scale bored steel pipe pile on a thin bearing layer”, Proc. 46th annual meeting of J.S.C.E., 1991, pp. 828-829.
[5] Nakai, T. “An isotropic hardening elastoplastic model for sand considering the stress path dependency in three-dimensional stresses”, Soils & Foundations, (29), 1, 1989, 119-137.
[6] Matsui, T. and N. Abe. “Multi-dimensional elasto-plastic consolidation analysis by finite element method”, Soils & Foundations (21), 1, 1981, 79-95
[7] Goodman, R.E., R.L. Taylor and T.L. Brekke, “A model for the mechanics of jointed rock”, ASCESM3, 1968, 637-659

Int. J. of GEOMATE, March, 2014, Vol. 6, No. 1 (Sl. No. 11), pp. 763-770.
MS No. 3167 received on July 03, 2013 and reviewed under GEOMATE publication policies.

Pertinent discussion including authors’ closure, if any, will be published in the March. 2015 if the discussion is received by Sept, 2014.
Corresponding Author: Kazuhiro Oda